ARTICLE

Study of (2, 0) Band of $A^2\Pi_u$-$X^2\Sigma_g^+$ System of N_2^+ by Optical Heterodyne Detected Velocity Modulation Spectroscopy

Yan-dan Wu[a,b], Jin-wen Ben[a], Ling Li[a], Li-juan Zheng[a], Yang-qin Chen[a], Xiao-hua Yang[a]*

a. Key Laboratory of Optical and Magnetic Resonance Spectroscopy, Ministry of Education, and Department of Physics, East China Normal University, Shanghai 200062, China; b. Department of Physics and Electronic Engineering, Hanshan Normal University, Chaozhou 521041, China

(Dated: Received on October 8, 2006; Accepted on January 29, 2007)

The (2, 0) band of the $A^2\Pi_u$-$X^2\Sigma_g^+$ system of N_2^+ was rotationally studied via optical heterodyne detected velocity modulation spectroscopy. Owing to the high sensitivity of the spectroscopy employed, the frequencies of 310 lines of this band were accurately determined. Moreover, those overlapped lines were also well determined via deconvolution method. A nonlinear least-squares fitting procedure using a standard Hamiltonian was applied to analyze this band. Therefore, the most accurate molecular constants were obtained.

Key words: N_2^+ molecular ion, Spectrum, Molecular constant

I. INTRODUCTION

The N_2^+ is one of the most important ions in the ionosphere, interstellar space and electric discharge plasma, so it has been extensively studied by many researchers using many different techniques. In 1923, Childs identified the $A^2\Pi$ state as a perturber of the first negative system [1]. In 1950, the $A^2\Pi_u$-$X^2\Sigma_g^+$ system of N_2^+ was first observed by Meinel in auroral emissions [2], thus, this system is also called Meinel system. Benesch *et al*. observed its (0, 0), (1, 0), (2, 0), (3, 0), (3, 1), (4, 1) and (4, 2) bands in hollow cathode discharge plasma [3]. Miller *et al*. detected the (4, 0) band by the laser-induced fluorescence technique (LIF) using a single-mode cw dye laser [4]. Ferguson *et al*. applied Fourier transform infrared spectroscopy to observe Doppler-limited emission spectra for the (0, 0), (1, 0), (0, 1) and (1, 2) bands of this system in a hollow cathode discharge plasma [5].

However, because the intensity of the spectrum of the neutral molecules can be several orders of magnitude larger than that of the ions, the spectrum of the ions is hard to observe. In 1983, Gudeman and co-workers first reported the use of velocity modulation laser spectroscopy (VMS) which is a very efficient method for recording high-resolution spectra of molecular ions while suppressing those due to neutrals [6]. In this technique, molecular ions are generated by ac discharging of the parent molecules, and meanwhile, the velocity of the produced ions is modulated by the ac discharge electric field. Therefore, the spectrum of molecular ions can be picked up by correlation detection methods at a lock-in amplifier due to the Doppler effect. This ions-selected spectroscopy accelerated the study of molecular ions and was applied to investigate the (7, 3) [7], (8, 3) [8], (6, 3) [9], (6, 1) and (13, 6) [10], (2, 5) [11], (12, 6) [12], (15, 8) [13], (9, 4) and (11, 5) [14], (2, 0), (3, 1), (4, 2), (7, 4), (7, 2) and (8, 5) [15], and (7, 4) and (7, 2) [16] bands of the N_2^+ Meinel system. Recently, Wang *et al*. developed optical heterodyne magnetic rotation enhanced VMS, OH-MR-VMS, for further improving the sensitivity [17]. The combined OH and MR techniques can reduce the noise due to the laser source, the discharge plasma and the high voltage pick-up of the discharge. Employing this newly developed technique, Wu *et al*. re-studied the (11, 5) and (12, 6) bands of N_2^+ *A*-*X* system [18].

Most of the studies on $A^2\Pi_u$-$X^2\Sigma_g^+$ of N_2^+ in the near-infrared region focused on analysis of the (2, 0) band by different techniques [15,19-21]. In this work, the (2, 0) band of $A^2\Pi_u$-$X^2\Sigma_g^+$ of N_2^+ in the region of 12400 cm^{-1} to 12800 cm^{-1} were re-observed by employing optical heterodyne detected velocity modulation spectroscopy (OH-VMS) [22]. Owing to the high signal-to-noise ratio of this spectroscopy, the frequencies of the spectra were accurately determined, and thus, it led to improved values for the molecular constants, more accurate by a factor about 3.

II. EXPERIMENTS

In this experiment, the velocity modulation and optical heterodyne detection techniques were used to eliminate the signals due to neutral species and to reduce the noise from both the laser source and the discharge. There were two kinds of modulation mechanisms employed: velocity modulation at the frequency of 37 kHz and frequency modulation at 500 MHz. The frequency

*Author to whom correspondence should be addressed. E-mail: xhyang@phy.ecnu.edu.cn, Fax: +86-21-62232056

modulation was implemented by phase modulating the incident laser beam with an electro-optic modulator (EOM).

The detailed description of the experiment can be found elsewhere [22]. Briefly, a single-mode Ti: sapphire autoscan laser (Coherent ring 899-29), pumped by a compact diode-laser-pumped Nd:YVO_4 laser (Coherent Verdi 10, @532 nm), was employed to record continuously a spectrum of N_2^+. The laser beam passed through an EOM driven at radio frequency 500 MHz for phase modulation, and then a sample cell. The transmitted light was detected by a PIN detector (ET-2030A) and converted to an electronic signal. The electronic output of the detector was demodulated by a double balance mixer (DBM) referring to the driven frequency of EOM at 500 MHz, and then further demodulated by a lock-in amplifier (Stanford SR830) referring to the velocity modulation frequency 37 kHz with a time constant of 100 ms. Finally, the dc output from the lock-in was processed by a computer as the laser was tuning. The N_2^+ ions were produced by Penning ionization in an ac glow discharge of nitrogen of 25 Pa with helium (99.999% purity) of 465 Pa as a buffer gas. The gas mixture flowed continuously through the water-cooled glass sample cell (50 cm in length and 1 cm in inner diameter) inside each end of which was located a pair of cylindrical copper electrodes. The discharge was driven at 37 kHz giving a current of 400 mA peak-to-peak as the velocity modulation. Additionally, a differential absorption spectrum of I_2 recorded simultaneously was used to calibrate the laser frequency with an absolute accuracy better than 0.007 cm^{-1}.

III. ANALYSIS

The effective Hamiltonian for the ground $X^2\Sigma_g^+$ state including the rotation, the centrifugal distortion and the spin-rotation interaction is

$$H(X^2\Sigma_g^+) = B_v(r)\mathbf{N}^2 - D_v(r)\mathbf{N}^4 + \gamma_v(r)\mathbf{N}\cdot\mathbf{S} \quad (1)$$

where, B_v is the rotational constant, D_v is the quartic centrifugal distortion constant, γ_v is the spin-rotation constant, $\mathbf{N}$ is the rotational angular momentum, $\mathbf{S}$ is the electronic spin-angular momentum, and r is the internuclear distance. This operator is diagonal within Hund's case (b), so it gives the expressions for the energy levels,

$$F_1(N) = B_vN(N+1) - D_v[N(N+1)]^2 + \frac{1}{2}\gamma_vN \quad (2)$$

$$F_2(N) = B_vN(N+1) - D_v[N(N+1)]^2 - \frac{1}{2}\gamma_v(N+1) \quad (3)$$

where the F_1 component corresponds to J=N+1/2 and F_2 corresponds to J=N–1/2.

The excited $A^2\Pi_u$ state approaches Hund's case (a) and its effective Hamiltonian is

$$H(A^2\Pi_u) = B_v(r)\mathbf{R}^2 + A(r)\mathbf{L}\cdot\mathbf{S} + \gamma(r)\mathbf{N}\cdot\mathbf{S} \quad (4)$$

where $\mathbf{R}$ denotes the nuclear rotational angular momentum, $\mathbf{L}$ the total electronic momentum, and A the interaction constant of $\mathbf{L}$ and $\mathbf{S}$. Let $\mathbf{J}$ be the total angular momentum, then $\mathbf{J}$=$\mathbf{R}$+$\mathbf{L}$+$\mathbf{S}$=$\mathbf{N}$+$\mathbf{S}$. The efficient Hamiltonian matrix elements are taken from Cramb *et al.* as follows [10]

$$\langle^2\Pi_{1/2}, J, v, e/f|H_{\rm eff}|^2\Pi_{1/2}, J, v, e/f\rangle = T_v - \frac{1}{2}A_v + (B_v - \frac{1}{2}A_{Dv} - D_v)x^2 + D_v(1-x^4) \mp (q_v + \frac{1}{2}p_v)x \quad (5)$$

$$\langle^2\Pi_{3/2}, J, v, e/f|H_{\rm eff}|^2\Pi_{3/2}, J, v, e/f\rangle = T_v + \frac{1}{2}A_v + (B_v + \frac{1}{2}A_{Dv})(x^2-2) - D_v(x^4 - 3x^2 + 3) \quad (6)$$

$$\langle^2\Pi_{1/2}, J, v, e/f|H_{\rm eff}|^2\Pi_{3/2}, J, v, e/f\rangle = -[B_v - 2D_v(x^2-1) \mp \frac{1}{2}q_vx](x-1)^{1/2} \quad (7)$$

$$\langle^2\Sigma^+, J, v, e/f|H_{\rm eff}|^2\Sigma^+, J, v, e/f\rangle = T_v + B_vx(x\mp1) - D_vx^2(x\mp1)^2 \pm\frac{1}{2}\gamma_v(x\mp1) \quad (8)$$

where the T_v is the vibrational energy and x=J+1/2, and the upper or lower signs ($\pm$ or $\mp$) refer to the e/f levels.

In the $A^2\Pi_u$ state, in addition to the previous constants, the spin-orbit coupling and the lambda-doubling are also taken into account through the molecular parameters A_v, A_{D_v}, p_v, and q_v. The molecular constants of the A state are highly correlated, so γ_v is set to zero, then T_v, B_v, A_v, and A_{D_v} become effective constants [4].

IV. RESULTS AND DISCUSSION

Among the lines observed in the region between 12400 and 12800 cm^{-1} with a signal-to-noise ratio up to 220, a total of 310 lines were assigned to 12 branches of the (2, 0) band of the $A^2\Pi_u$-$X^2\Sigma_g^+$ of the N_2^+ ion with J values up to 35.5, which are listed in Table I and Table II. A partial spectrum of the (2, 0) band is shown in Fig.1. The observed line shape is the second derivation of the Gaussian profile [22]. The center wavelength of the line can be precisely determined by line profile fitting. In the N_2^+ $A^2\Pi_u$-$X^2\Sigma_g^+$ system, branches with common upper states are very close, such as the pairs of P_{11ee}/Q_{12ef}, Q_{11fe}/R_{12ff}, P_{21ee}/Q_{22ef}, and Q_{21fe}/R_{22ff}, since their separations depend only on the spin splitting of the ground state $X^2\Sigma_g^+$. It is

DOI:10.1088/1674-0068/20/3/285-290

TABLE I Wavenumber (in cm^{-1}) of the observed lines of the (2, 0) band of the $A^2\Pi_u$-$X^2\Sigma_g^+$ system of N_2^+

J	P_{11}	P_{22}	Q_{11}	Q_{22}	R_{11}	R_{22}
0.5				12768.0046(−126)	12698.8075(3)	12773.2316(51)
1.5		12760.3343[a](−25)[b]	12694.9450(−130)	12765.5380(50)	12703.2605(−1)	12774.2250(108)
2.5	12687.2500(−139)	12754.0075(−52)	12695.5730(60)	12762.6630(−92)	12707.1881(−31)	12774.8150(−85)
3.5		12747.2977(−144)[c]	12695.6580(41)	12759.4316(−21)	12710.5978(26)	12775.0500(−30)
4.5	12680.2700(−8)	12740.2378(36)	12695.2210(8)	12755.8104(−60)	12713.4934(38)	12774.8975(−32)
5.5	12675.9837(90)	12732.7845(68)	12694.2700(25)	12751.8142(−43)[c]	12715.8579(−28)	12774.3630(−15)
6.5	12671.1921(−39)	12724.9426(15)	12692.7946(−34)	12747.4361(−20)	12717.7196(39)	12773.4517(97)
7.5	12665.8778(−49)	12716.7273(49)	12690.8165(27)	12742.6751(21)	12719.0435(−134)	12772.1358(53)
8.5	12660.0478(−74)[c]	12708.1230(34)	12688.3200(26)	12737.5235(28)	12719.8807(−60)	12770.4313(40)
9.5	12653.7169(8)	12699.1227(−75)	12685.3120(4)	12731.9813(26)	12720.2076	12768.3282(−13)
10.5	12646.8705(25)	12689.7539(21)	12681.8038(48)	12726.0466(23)	12720.0241(17)	12765.8348(5)
11.5	12639.5138	12679.9859(40)	12677.7827(4)	12719.7139(−9)	12719.3353(18)	12762.9341(−45)
12.5	12631.6575(11)	12669.8245(67)	12673.2510(−135)	12712.9830(−44)	12718.1378(−59)	12759.6367(−29)
13.5	12623.3010(23)	12659.2572(3)	12668.2551(70)	12705.8522(−72)	12716.4588(34)	12755.9322(−23)
14.5	12614.4420(−15)	12648.3065(100)	12662.7308(−53)	12698.3288(8)	12714.2739(27)	12751.8142(−61)[c]
15.5	12605.0915(−24)	12636.9337(−4)	12656.7305(−5)	12690.3929(22)	12711.5954(18)	12747.2977(32)[c]
16.5	12595.2513(−11)	12625.1669(−2)	12650.2361(7)	12682.0489(41)	12708.4232(−15)	12742.3459(−85)
17.5	12584.9189(−31)	12612.9960(28)	12643.2530(12)	12673.2810(−69)	12704.7631(−39)	12736.9998(23)
18.5	12574.0975(−76)	12600.4099(−2)	12635.7795(−30)	12664.1199(23)	12700.6204(−19)	12731.2201(−14)
19.5	12562.8038(−4)	12587.4193(38)	12627.8398(99)	12654.5307(−11)	12695.9934(5)	12725.0217(−24)
20.5	12551.0196(23)	12573.9974(−99)	12619.3907(−52)	12644.5266(−17)	12690.8866(62)[c]	12718.4067(36)
21.5	12538.7570(−32)	12560.1820(−15)	12610.4793(−33)	12634.1134(83)	12685.2810(−57)	12711.3619(54)
22.5	12526.0178(−37)	12545.9394(−30)	12601.0920	12623.2630(27)	12679.2153(18)	12703.8796(−29)
23.5	12512.8111(34)	12531.2814(−8)	12591.2252(−5)	12611.9970(49)	12672.6681(60)	12695.9751(−41)
24.5	12499.1377(169)	12516.2048(35)	12580.8828(27)	12600.2998(8)	12665.6394(53)	12687.6443(−7)
25.5	12484.9605(−20)	12500.6921(−60)	12570.0639(90)	12588.1778(−15)	12658.1276(31)	12678.8711(−72)
26.5	12470.3290(−56)		12558.7860(−33)	12575.6202(−114)	12650.1411(−122)	12669.6727(−49)
27.5	12455.2402(15)	12468.4197(1)	12547.0385(24)	12562.6537(−9)	12641.6998(−30)	12660.0478(63)[c]
28.5	12439.6791(29)		12534.8172(26)	12549.2467(−4)	12632.7783(−21)	12649.9609(78)
29.5	12423.6538(51)		12522.1285(26)	12535.4097(19)		
30.5	12407.1567(−6)		12508.9719(8)	12521.1355(−2)		
31.5			12495.3619(106)	12506.4302(5)		
32.5			12481.2680(6)	12491.2774(−116)		
33.5			12466.7335(132)			
34.5			12451.7128(21)	12459.6970(29)		
35.5			12436.2369(−27)			

[a] Numbers in parentheses denote the differences of the observed and calculated in units of the last quoted digits.
[b] Severely overlapped lines assigned to two transitions.
[c] Numbers denote the observed.

very difficult to determine the spectral positions of the severely overlapped lines at low J. Therefore, such lines were accurately determined by a deconvolution method according to their line shape function, linewidth and the intensity distribution of the branches. The result of such deconvolution is illustrated in Fig.2.

The experimental lines were least-squares analyzed. The determinations of spectral positions were occasionally affected by the too weak intensity, the asymmetry of the line shape and the overlap of the lines. The initial weights were calculated from the expression $w=1/\delta^2$, where δ was the estimated uncertainty of the spectral positions varying from 0.002 cm^{-1} to 0.01 cm^{-1}. Finally, the weights were evaluated as Ref.[23] did for fitting, and the convergent standard deviation 0.0036 cm^{-1}, half of our experimental error of 0.007 cm^{-1}, was obtained. The molecular constants determined are listed in Table III, and those of previous works are also

DOI:10.1088/1674-0068/20/3/285-290

TABLE II Wavenumber (in cm^{-1}) of the observed lines of the (2, 0) band of the $A^2\Pi_u$-$X^2\Sigma_g^+$ system of N_2^+

J	P_{12}	P_{21}	Q_{12}	Q_{21}	R_{12}	R_{21}
0.5				12771.8506(−66)	12694.9627(−91)	12777.0576(43)
1.5			12687.2857(−12)	12773.2150(23)	12695.6020(120)	12781.8809(87)
2.5	12675.7352(−227)	12765.5140(40)	12684.0587(−18)	12774.1960(48)	12695.6840(−21)	12786.3158(30)
3.5	12668.6886(7)	12762.6260(-140)	12680.3150(29)	12774.7890(−23)	12695.2650(34)	12790.3686(−49)
4.5	12661.0946(−22)	12759.3850(−73)	12676.0471(38)	12775.0080(−36)	12694.3190(9)	12794.0576(53)
5.5	12652.9897(34)	12755.7550(−108)	12671.2655(97)	12774.8407(−94)	12692.8600(23)	12797.3532(61)
6.5	12644.3587(2)	12751.7531(−56)	12665.9528(11)	12774.3040(−7)	12690.8866(39)[a]	12800.2603(51)
7.5	12635.2148(−9)	12747.3700(9)	12660.1345(11)	12773.3767(37)	12688.4060(104)	12802.7687(54)
8.5	12625.5553(−50)	12742.5914(−34)	12653.8103(69)	12772.0458(−65)	12685.4013(23)	
9.5	12615.3977(24)	12737.4284(−49)	12646.9655(10)	12770.3479(80)	12681.8965(10)	
10.5	12604.7245(10)	12731.8793(−28)	12639.6172(−24)	12768.2281(−49)	12677.8827(−54)	
11.5	12593.5518(39)	12725.9362(−23)	12631.7655(−58)	12765.7281(−4)	12673.3806(12)	
12.5	12581.8718(2)	12719.6042(44)	12623.4221(−7)	12762.8141(−96)	12668.3780(57)	
13.5	12569.6940(−37)	12712.8663(30)	12614.5755(−14)	12759.5167(12)	12662.8681(−14)	
14.5	12557.0332(41)	12705.7271(11)	12605.2246(−118)	12755.7959(−52)	12656.8723(−13)	
15.5	12543.8696(6)	12698.1854(−1)	12595.3998(44)	12751.6730(−48)	12650.3896(24)	
16.5	12530.2223(20)	12690.2378(−11)		12747.1459(31)	12643.4181(54)	
17.5	12516.0947(88)	12681.8700(−138)	12574.2660(−92)	12742.1877(−58)	12635.9480(−47)	
18.5	12501.4560(−124)	12673.1234(57)	12562.9839(3)	12736.8273(−1)	12628.0133(41)	
19.5	12486.3715(9)	12663.9400(17)	12551.2080(−24)	12731.0466(44)	12619.5825(−19)	12801.5628(−4)
20.5	12470.7960(11)	12654.3383(−50)	12538.9555(−25)	12724.8375(20)		12798.7509(−62)
21.5	12454.7382(−57)	12644.3200(−106)	12526.2296(12)	12718.2100(47)	12601.3022(33)	12795.5287(55)
22.5		12633.9014(32)	12711.1518(22)	12591.4504(85)	12791.8563(−32)	
23.5		12623.0352(−90)		12703.6641(−23)	12581.1096(−12)	
24.5		12611.7685(17)	12485.1973(3)	12695.7599(60)	12570.3007(−67)	
25.5			12470.5790(7)	12687.4125(20)		
26.5			12455.4954(38)	12678.6326(−20)		

[a] Severely overlapped lines assigned to two transitions.

TABLE III Molecular constants (in cm^{-1}) of the (2, 0) band of the $A^2\Pi_u$-$X^2\Sigma_g^+$ system of N_2^+

		This work	Ref.[20]	Ref.[19]	Ref.[15]
$X^2\Sigma_g^+$	B_0	1.9223897(53)[a]	1.922364(24)	1.922384(14)	1.922366[b]
	$D_0\times10^6$	5.9748(50)	6.011(55)	5.9479(82)	5.941[b]
	$\gamma_0\times10^3$	9.1965(90)	9.287(37)	9.203(35)	9.316[b]
$A^2\Pi_u$	B_2	1.6973871(53)	1.697360(21)	1.697384(14)	1.6973673(17)
	$D_2\times10^6$	5.9609(50)	5.986(51)	5.9368(81)	5.9319(14)
	A_2	−74.63428(23)	−74.63529(54)	−74.63628(79)	−74.63666(73)
	$A_{D_2}\times10^5$	−7.142(73)	−6.72(44)	−7.05(20)	−6.06(18)
	$p_2\times10^3$	5.118(14)	5.173(82)	4.878(44)	5.017(44)
	$q_2\times10^4$	−3.3696(50)	−3.345(69)	−3.298(10)	−3.336(13)
T_{20}		12732.84033(13)	12732.83583(31)	12732.8463(4)	12732.83795(40)
Lines		310	108	376	367
σ		0.0036	0.0015	0.632	0.0041

[a] Numbers in parentheses denote one standard deviation in units of the last quoted digits.
[b] Fixed at the values of Ref.[5].

DOI:10.1088/1674-0068/20/3/285-290

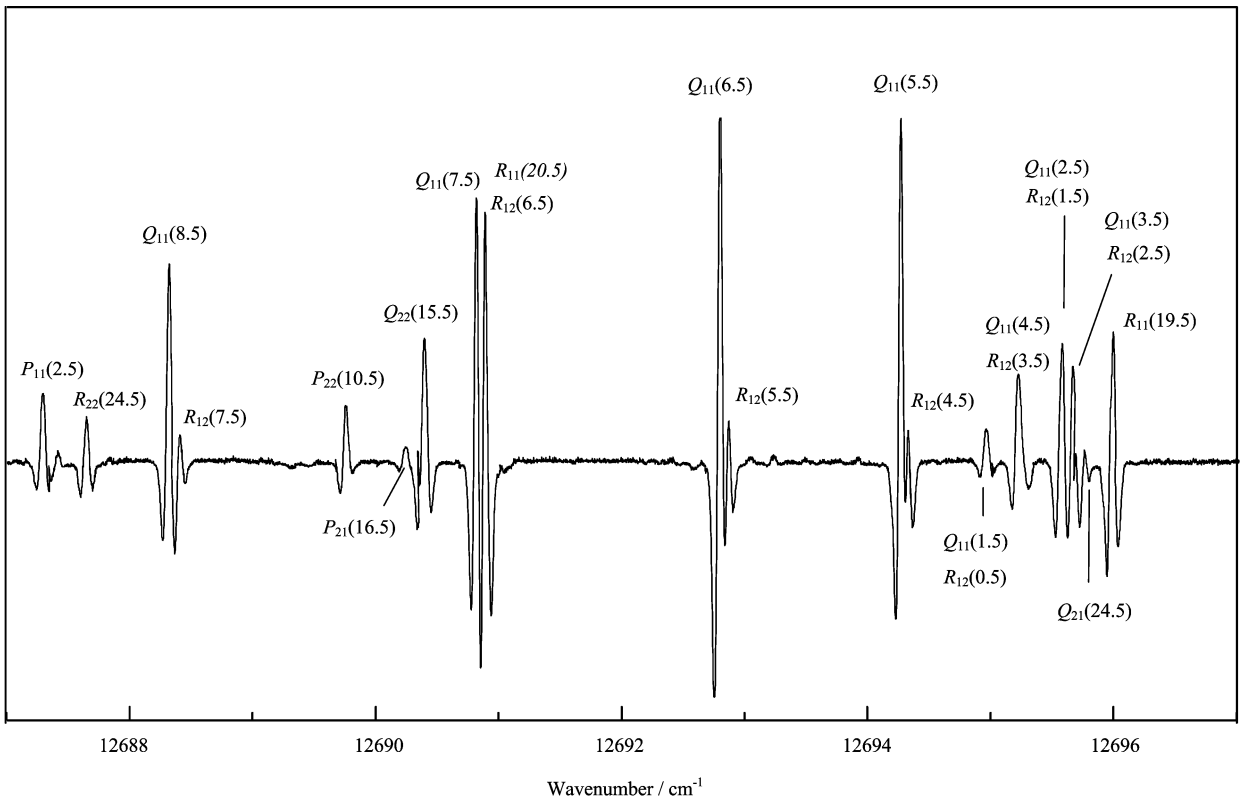

FIG. 1 Part of the N_2^+ $A^2\Pi_u$-$X^2\Sigma_g^+$ (2, 0) spectrum near the Q_{11}-branch and R_{12}-branch heads.

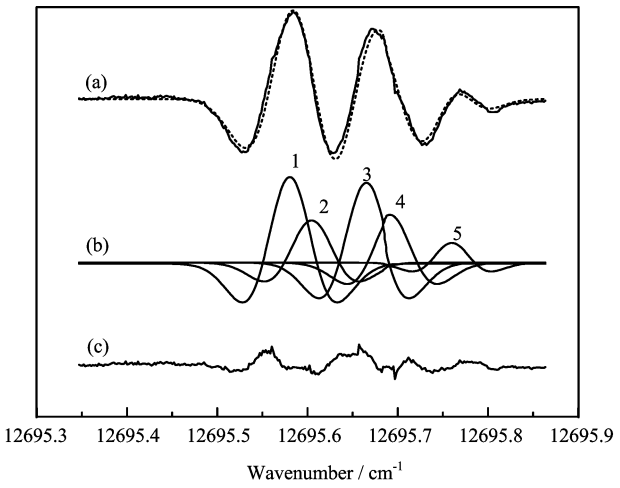

FIG. 2 Deconvolution of the overlapping lines. Trace (a) shows the experimental line (dashed) and the fitted one (solid). Trace (b) shows the experimental line and the result of the PeakFit program (five decomposed peaks). Trace (c) shows the residuals between the fitting and the experimental ones. Line identification: 1: $Q_{11}(2.5)$, 2: $R_{12}(1.5)$, 3: $Q_{11}(3.5)$, 4: $R_{12}(2.5)$ and 5: $Q_{21}(24.5)$.

listed for comparison. Most constants are in good agreement with the previous literature within 3σ uncertainty except the band origin. The present results represent improvements in some constants, compared with the most accurate constants of Ref.[19], e.g., by a factor of 3 for B_0 and B_2, a factor of 2 for D_0 and D_2, and a factor of 4 for A_2 and γ_0. That some constants of the $A^2\Pi_u$ state of Collet *et al.* [15] seem more accurate than ours is just because their constants of the ground state were fixed at the result of Ferguson *et al.* [5] which was obtained via the spectrum in the same frequency region, thus are not actually more accurate. Following a similar procedure, seemingly more accurate constants of the A state were obtained when we tried our fitting procedure with the constants of the X state fixed, just like Collet *et al.* did. We, therefore, believe our constants obtained are the most accurate so far.

V. CONCLUSION

Employing OH-VMS, the spectrum of (2, 0) band of N_2^+ $A^2\Pi_u$-$X^2\Sigma_g^+$ system ranging from 12400 cm^{-1} to 12800 cm^{-1} was observed with high signal-to-noise ratio up to 220. 310 rotationally spectral lines were accurately determined. Moreover, overlapping lines were also well determined by a deconvolution method. In addition, they were correctly assigned to 12 branches of this band, and thus the most accurate molecular constants were obtained via a nonlinear least-squares fitting procedure. The values of these constants are improved

DOI:10.1088/1674-0068/20/3/285-290

by a factor of approximate 3.

VI. ACKNOWLEDGMENTS

This work was supported by the National Natural Science Foundation of China (No.10574045 and No.10434060), and the National Key Basic Research and Development Program of China (No.2006CB921604).

[1] W. H. J. Childs, Proc. R. Soc. London Ser. A **137**, 641 (1932).
[2] A. B. Meinel, Astrophys J. **112**, 562 (1950).
[3] W. Benesch, D. Rivers, and J. Moore, J. Opt. Soc. Am. **70**, 792 (1980).
[4] T. A. Miller, T. Suzuki, and E. Hirota, J. Chem. Phys. **80**, 4671 (1984).
[5] D. W. Ferguson and K. N. Rao, J. Mol. Spectrosc. **153**, 599 (1992).
[6] C. S. Gudeman and R. J. Saykally, Annu. Rev. Phys. Chem. **35**, 387 (1984).
[7] M. B. Radunsky and R. J. Saykally, J. Chem. Phys. **87**, 898 (1987).
[8] B. Lindgren, P. Royen, and M. Zackrisson, J. Mol. Spectrosc. **146**, 343 (1991).
[9] I. H. Bachir, T. R. Huet, and J. L. Destombes, J. Mol. Spectrosc. **170**, 601 (1995).
[10] D. T. Cramb, A. G. Adam, D. M. Steunenberg, A. J. Merer, and M. C. L. Gerry, J. Mol. Spectrosc. **141**, 281 (1990).
[11] D. T. Cramb, M. C. L. Gerry, F. W. Dalby, and I. Ozier, Chem. Phys. Lett. **178**, 115 (1991).
[12] A. Al-Khalili, H. Ludwigs, and P. Royen, J. Mol. Spectrosc. **183**, 200 (1997).
[13] A. Al-Khalili, H. Ludwigs, and P. Royen, Chem. Phys. Lett. **284**, 191 (1998).
[14] B. Lindgren, P. Royen, and M. Zackrisson, J. Mol. Spectrosc. **156**, 319 (1992).
[15] D. Collet, J. L. Destombes, I. Hadj Bachir, and T. R. Huet, Chem. Phys. Lett. **286**, 311 (1998).
[16] Y. Y. Liu, C. X. Duan, S. H. Wu, H. Zhuang, and Y. Q. Chen, J. Mol. Spectrosc. **208**, 144 (2001).
[17] R. J. Wang, Y. Q. Chen, P. P. Cai, J. J. Lu, Z. Y. Bi, X. H. Yang, and L. S. Ma, Chem. Phys. Lett. **307**, 339 (1999).
[18] S. H. Wu, Y. Q. Chen, H. Zhuang, X. H. Yang, Z. Y. Bi, L. S. Ma, and Y. Y. Lu, J. Mol. Spectrosc. **209**, 133 (2001).
[19] I. H. Bahir, H. Bolvin, C. Demuynck, J. L. Destombes, and A. Zellagui, J. Mol. Spectrosc. **166**, 88 (1994).
[20] K. Harada, T. Wada, and T. Tanaka, J. Mol. Spectrosc. **163**, 436 (1994).
[21] K. Harada and T. Tanaka, Chem. Phys. Lett. **227**, 651 (1994).
[22] G. L. Chen, X. H. Yang, X. P. Ying, G. Liu, Y. X. Huang, and Y. Q. Chen, Chin. Sci. Bull. **49**, 2354 (2004).
[23] L. J. Zheng, X. H. Yang, L. Wu, K. Kaniki, Y. C. Guo, Y. Y. Liu, and Y. Q. Chen, J. Mol. Spectrosc. **226**, 81 (2004).

DOI:10.1088/1674-0068/20/3/285-290